

SMR 용 고성능 구조재료 개발 현황 at KAIST

Development of advanced structural materials for SMRs at KAIST – Recent progress

Changheui Jang (장창희)

**김현명, 김채원, 허웅, 신지호, 엄현준,
Gokul Obulan Subramanian, 안태정**

Oct. 2021

chjang@kaist.ac.kr (<http://nurmat.kaist.ac.kr/>)

(042)350-3824

NQE, KAIST

Intro: water-cooled SMRs

D. Sandusky et al., PNNL report no.22290 (2013)

Materials

• NuScale

- Almost same as PWR
- May adopt 3DP RPV

• i-SMR

- Bigger than NuScale
- Weight reduction is issue

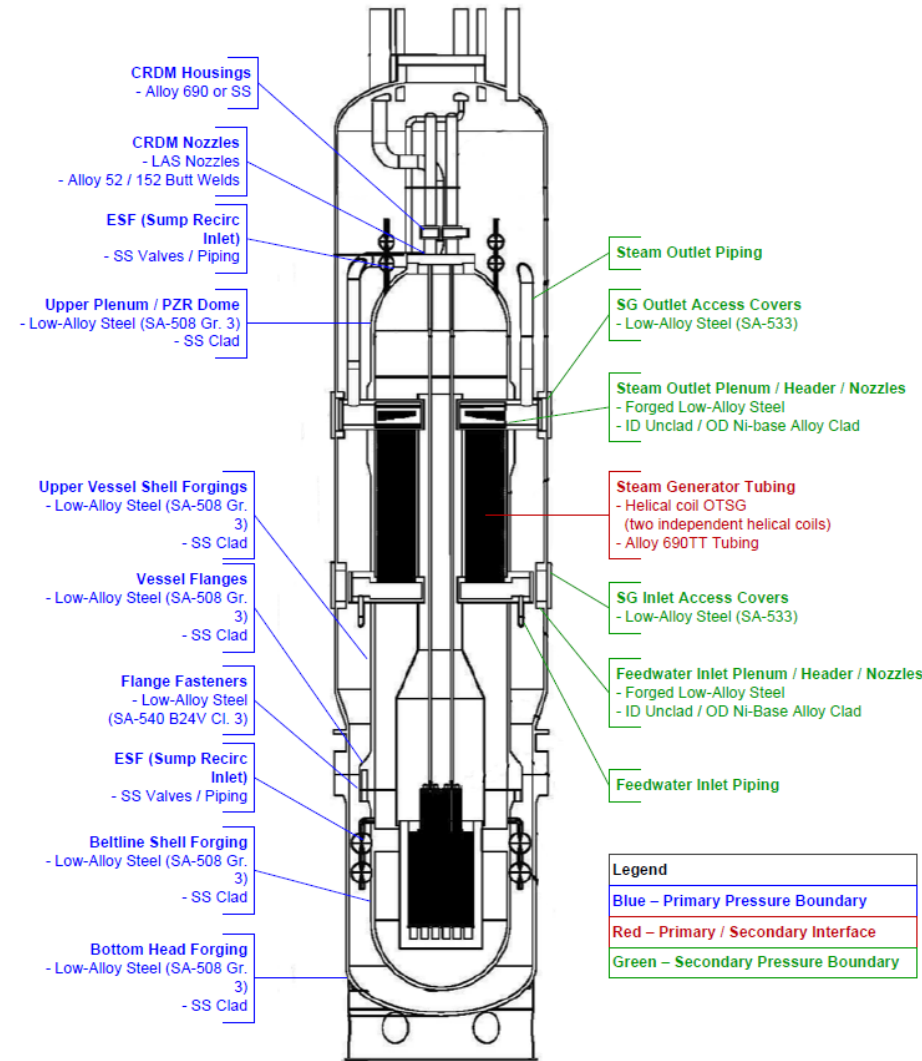
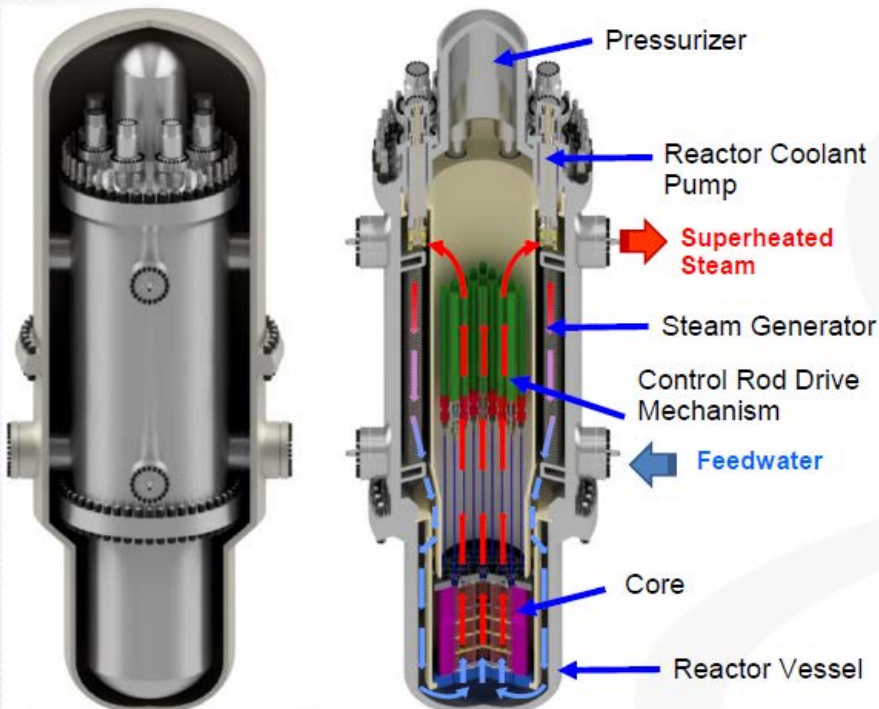


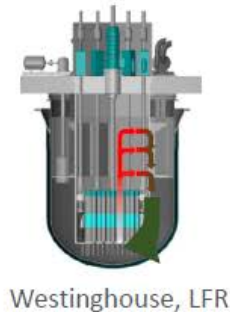
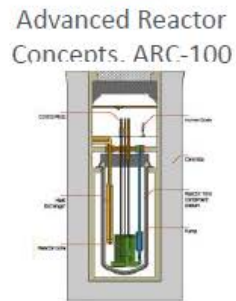
Figure 5-2 NuScale Section Drawing with Pressure Boundary Components Annotated

Intro: non-water cooled SMRs

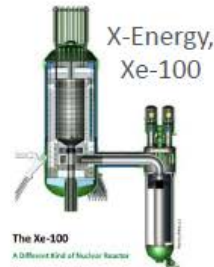
S. Sham, Section III, Division 5 Overview, presented at ASME Div.5 WS, Nov. 8-9, 2020

Examples of Different Advanced Reactor Designs Being Developed By Industry

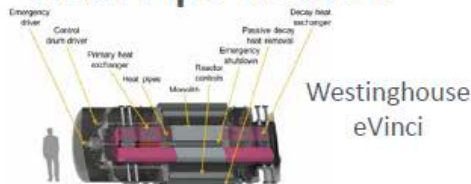
Fast Reactors



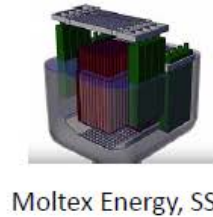
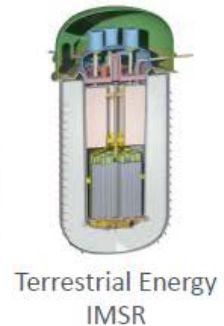
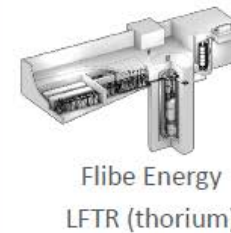
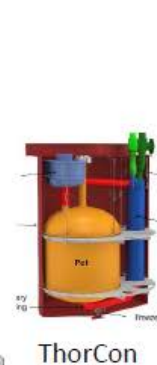
Gas Reactors



Heat Pipe Reactor



Molten Salt Reactors



Intro: Materials Requirements

❑ Very High-Temperature Reactors:

~ 900 °C with He

Thermal neutron spectrum

❑ Fast Reactors:

~ 550 °C with liq. Na/water/S-CO₂

~ 700 °C with LBE or Molten Salts

Fast neutron spectrum

❑ Light Water Reactors:

~ 300 °C with water

Thermal neutron spectrum

Research in Nu_HTML

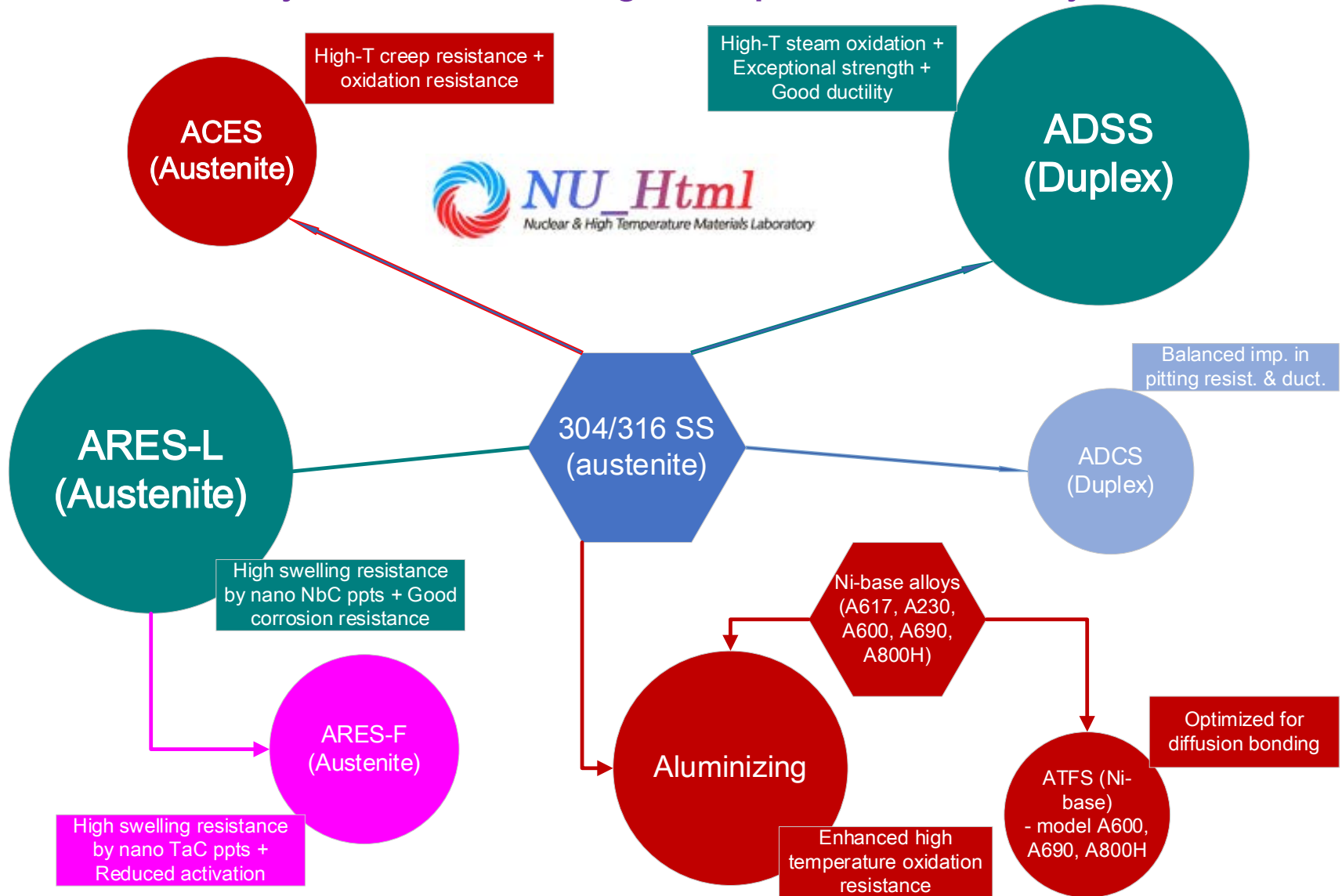
High
Temperature
Strength

Corrosion
Resistance

Radiation
Resistance

Intro: Tree of Advanced Alloys in Nu_HTML

A2S Alloys for Nuclear & High-Temperature Power Systems



I. ADSS

for LWR & HTR

ADSS - Motivation

❑ Zr-based Fuel Cladding

- Low neutron c-x
- Poor Corrosion Resistance

Zr Cladding oxidation: **Major source**
of **hydrogen** generation



Absorption c-x (barns)

Co : 37.2

Ni : 4.43, Cr : 3.1, Fe : 2.55

Na : 0.53

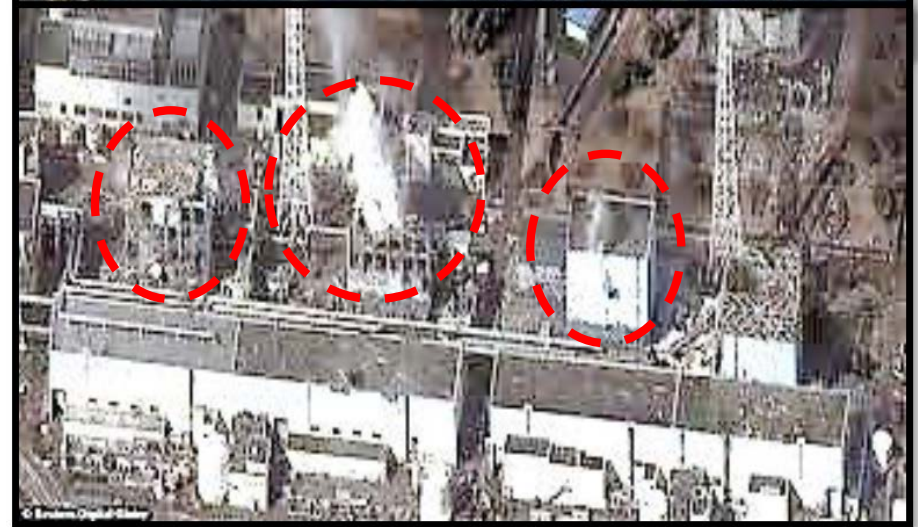
Al : 0.242

Zr : 0.185, Pb, Si : 0.171

Mg : 0.063

Be : 0.0092

C : 0.0035



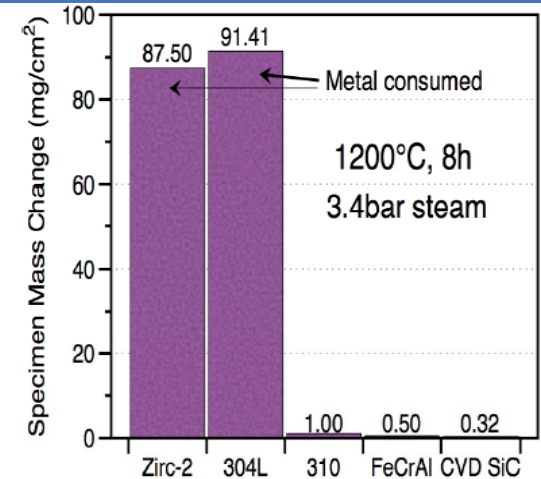
Better materials than Zr-alloys??

ADSS - Motivation

❑ Current issues of candidate ATF materials

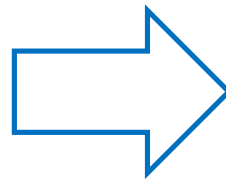
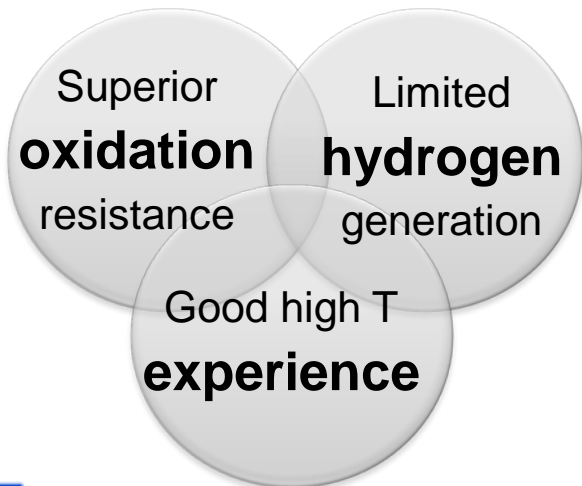
- **Ceramic** cladding (SiC)
 - **Brittle fracture** in normal operation
 - Fission products **retention issue**
- **Coating** on Zr-alloy (Cr/Zr)
 - Inherent Zr behaviors (**balloon/burst**)
- **Metallic** cladding (Mo, FeCrAl)
 - **Poor oxidation** (Mo) / **Embrittlement** (FeCrAl)

❑ Concept of ADSS alloys

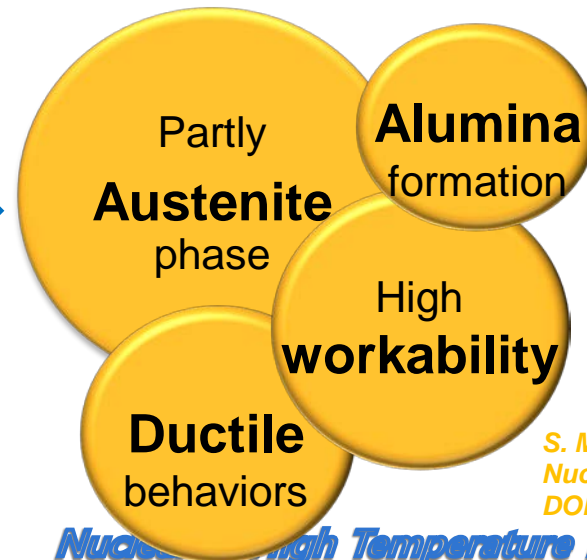


▲ A comparison of conventional alloys and ATF candidate materials in high temp. steam oxidation

Advanced Steel



ADSS alloy



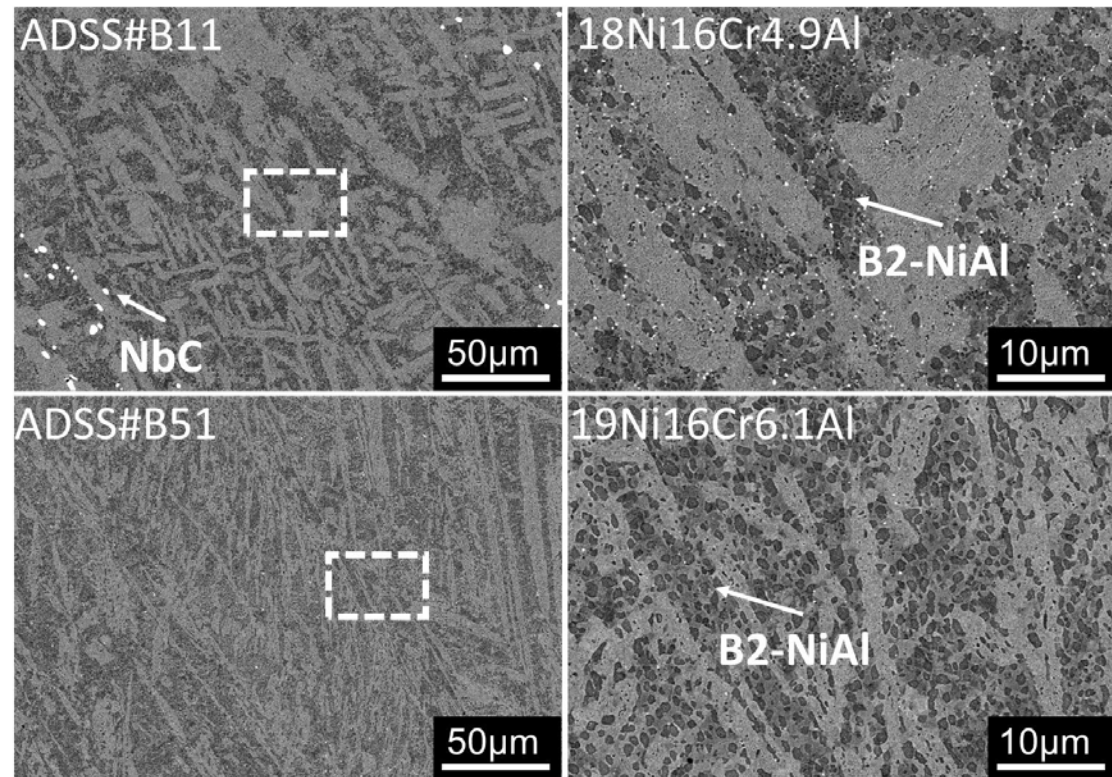
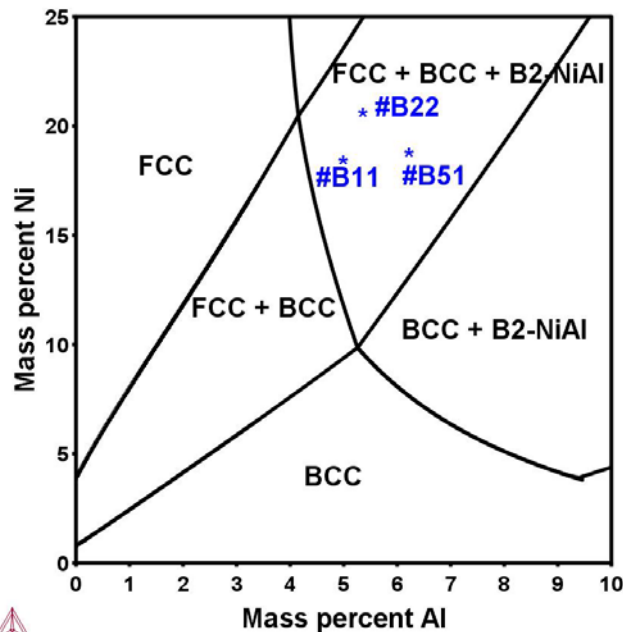
S. Maloy et. al., Adv. in Nucl. Fuel and Mater. DOE Purdue WS, 2014

ADSS – Composition and microstructure

H. Kim et al. J. Nucl. Mater., 507 (2018) 1

Thermodynamic modeling

- Fe-(16-20)Ni-16Cr-(5.5-7.0)Al + (Nb, Mn, C, Si)
- **Austenite(FCC), ferrite(BCC), nickel aluminide (B2-NiAl) co-exist**
- B2-NiAl phase fraction/stability depends on Ni/Al, respectively

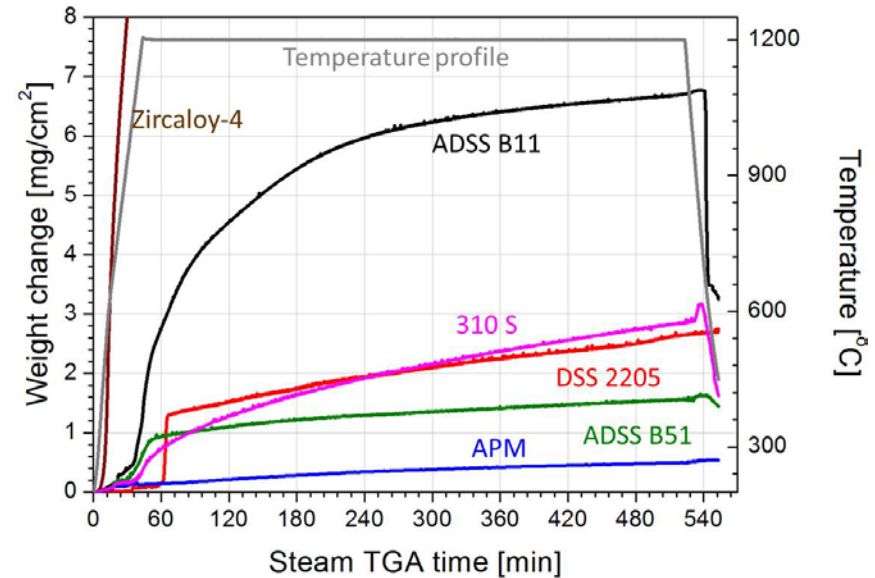


▲ Thermo-Calc phase diagram (TCFE-9 database) for Fe-16Cr-xAl-yNi system at 900°C, and the indicated target ADSS compositions.

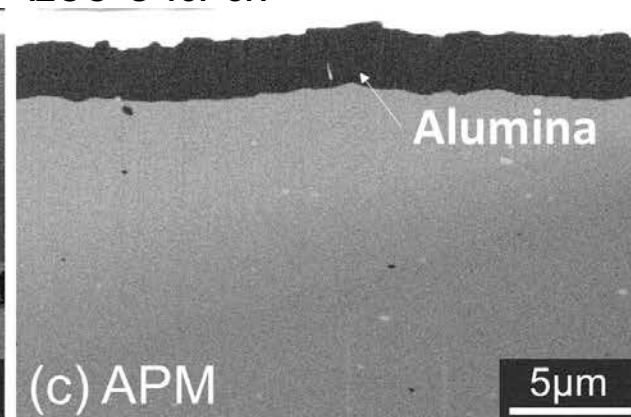
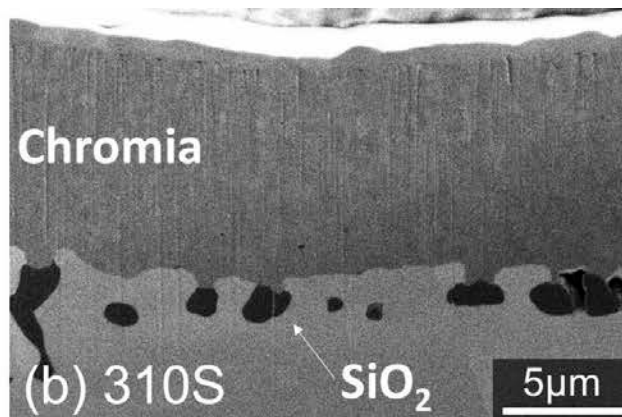
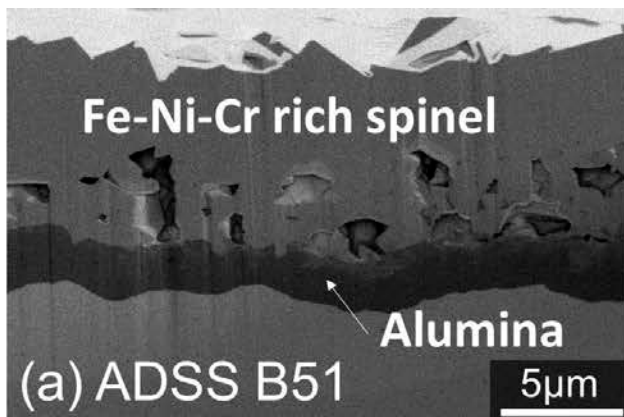
Complex Microstructure!

High temperature steam oxidation

- Steam TG 1200°C 8h
- ADSS alloys showed somewhat larger weight gain, but with similar kinetics at steady-state
 - Confirmed to form protective alumina formation, comparable to FeCrAl alloys



▲ Steam TG graph of ADSS and reference alloys at 1200°C for 8h



▲ Cross-sectional oxide FIB/SEM images for ADSS alloys (a) B51, (b) 310 S, and (c) APM stainless steels after exposure in steam TG at 1200 °C for 8 h.

□ PWR corrosion

- ADSS alloys showed weight gain in PWR

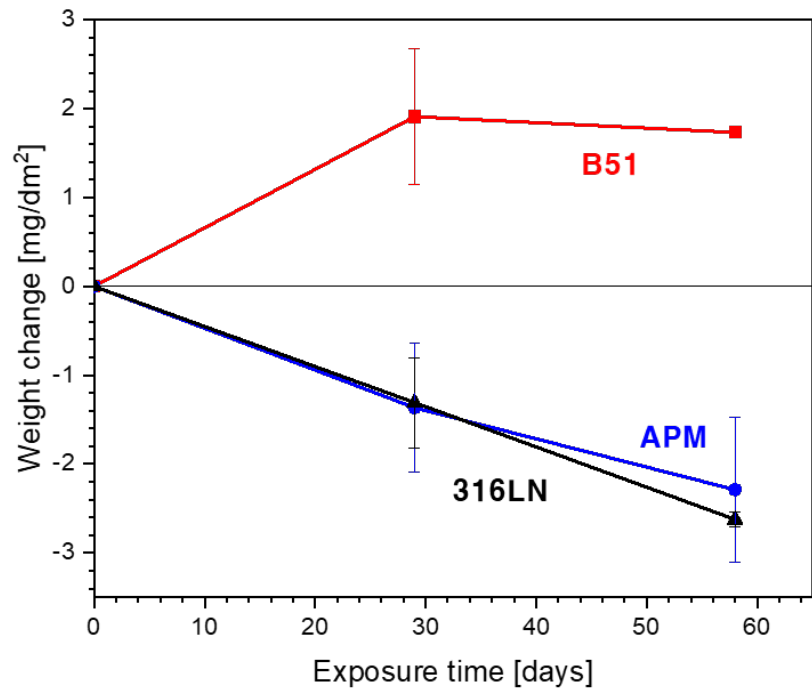
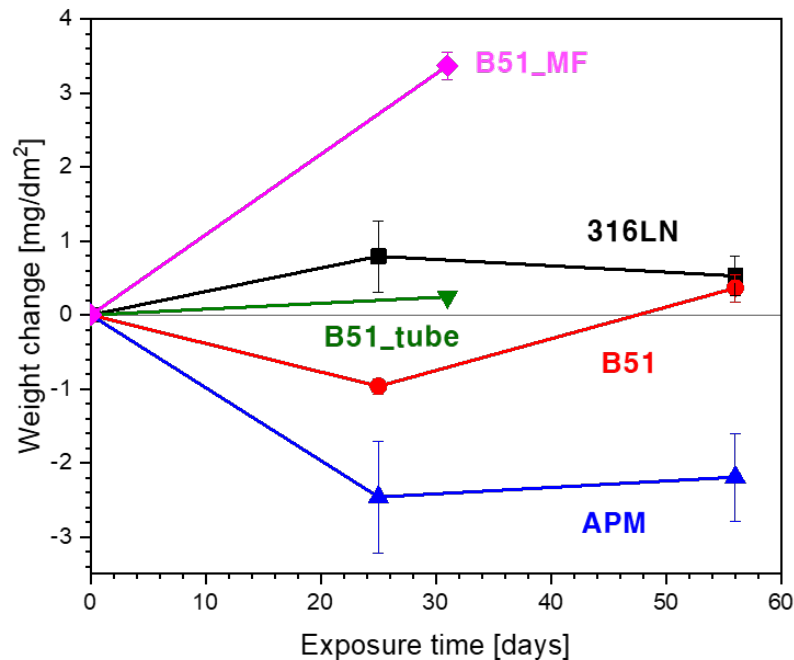
Table 6

Mass gain and oxide thickness after 30 days corrosion in the simulated PWR environment.

Materials	Mass gain [$\text{mg} \cdot \text{dm}^{-2}$]	Oxide thickness [μm]
ADSS alloys	0.62 ± 0.30	0.05–0.15
APM	-0.33 ± 0.06	—
310 S	Negligible ^a	<0.01
Zircaloy-4	20–30	1.3–2.0 ^b

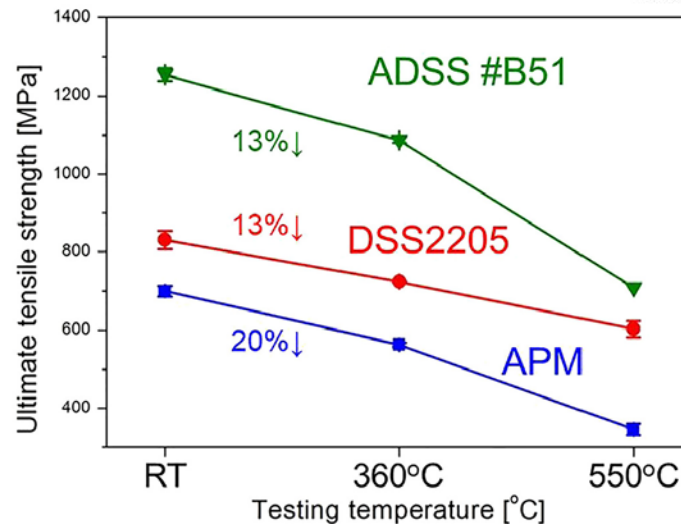
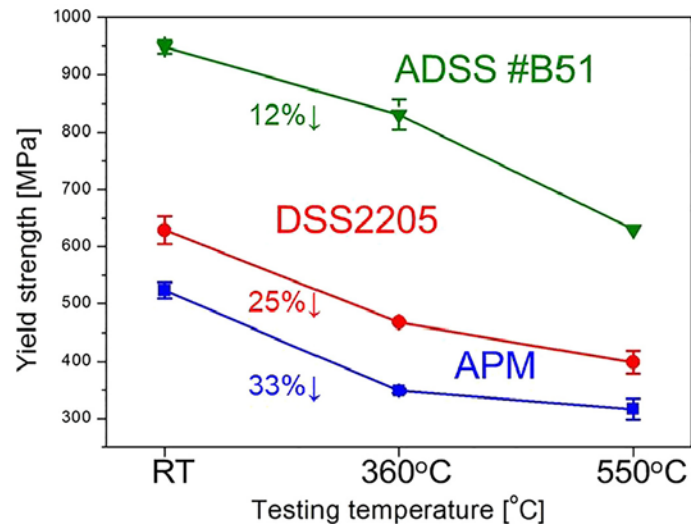
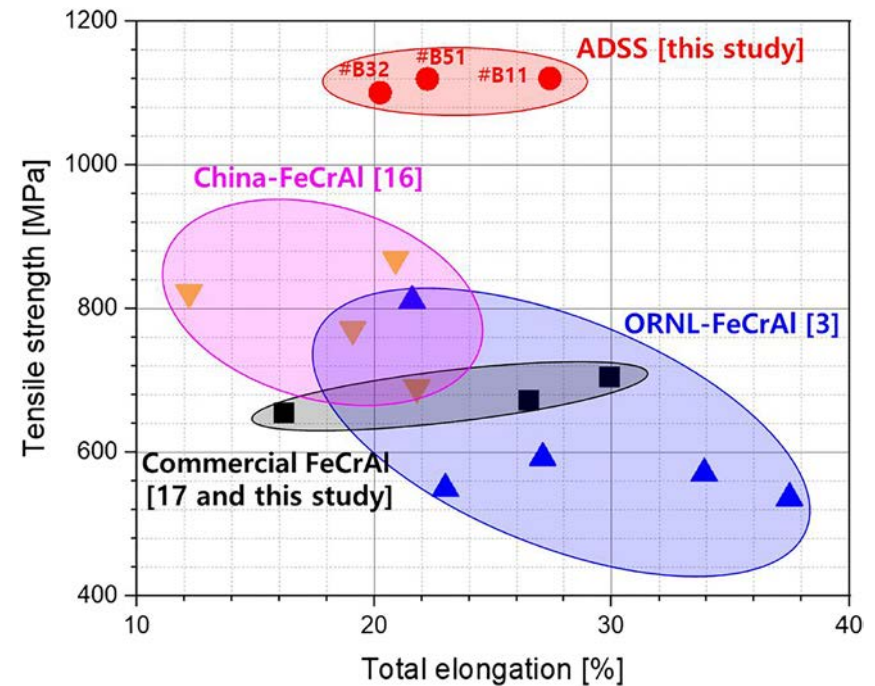
^a Mass gain less than 0.03 mg dm^{-2} .

^b Values estimated from the longer-term data.



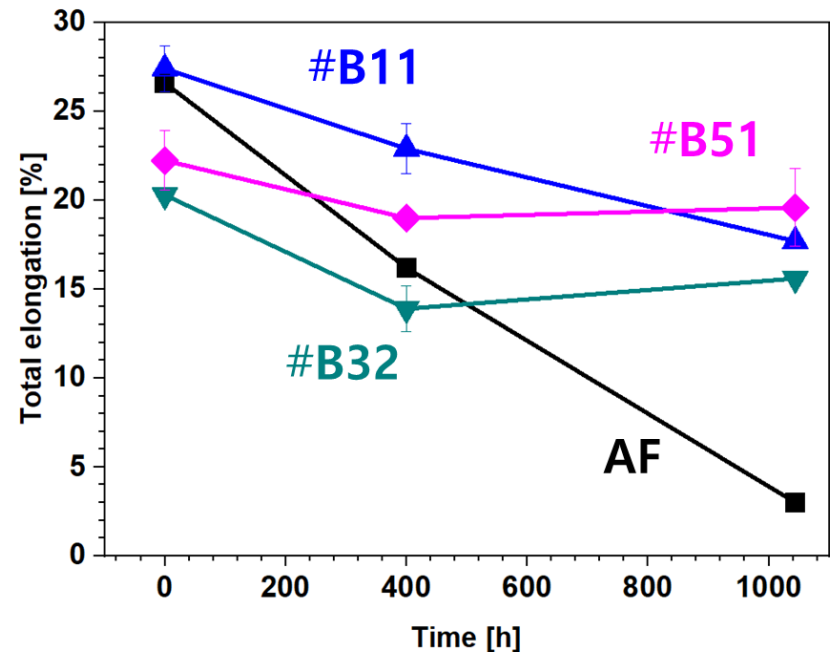
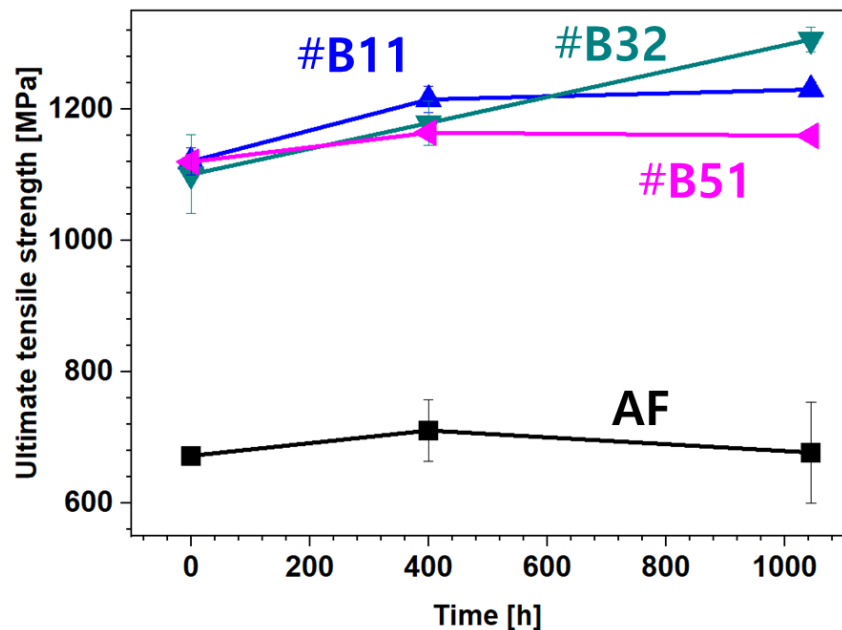
▲ Simulated PWR immersion corrosion test (left) at 320 °C in 150 bar and (right) at 360 °C in 190 bar

□ Mechanical properties



425 °C thermal aging for up to 1 kh

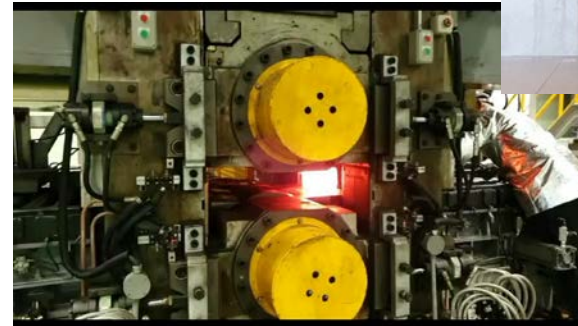
- All Fe-based alloys, embrittlement ($YS \uparrow$, elongation \downarrow)
- The degree of thermal aging, $ADSS \ll AF$
 - Due to austenite phase in ADSS
- Austenite phase : $ADSS \#B11 > ADSS \#B32$
- Degree of thermal aging : $ADSS \#B11 < ADSS \#B32$



▲ YS and total elongation of ADSS alloys and AF after thermal aging at 425 °C for up to 1 kh

ADSS - Fabrication of thin tubes

❑ Fabrication of thin ADSS tubes



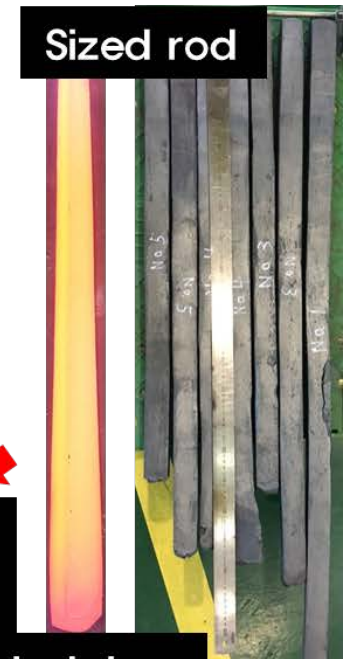
As-cast ingots



Sizing by hot forging
and/or rolling



Sized rod



Fabricated bar
(master bar)



Thin tube
1.6m O.3t

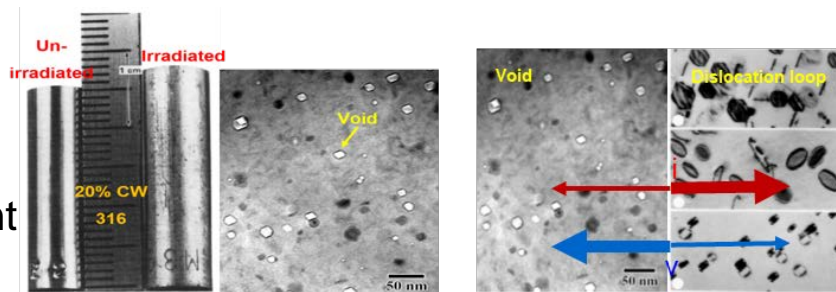


II. ARES

for LWR & HTR

Material degradation in current LWRs

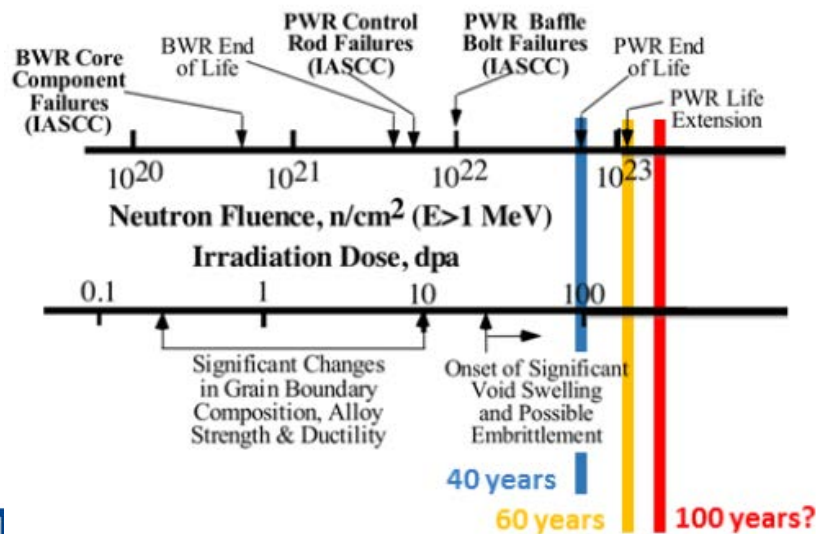
- Stress Corrosion Cracking (SCC)
- **Irradiation Assisted SCC (IASCC)**
- **Radiation induced segregation**
 - Cr, Mo depletion / Ni, Si and P enrichment
- Radiation hardening
- Irradiation creep



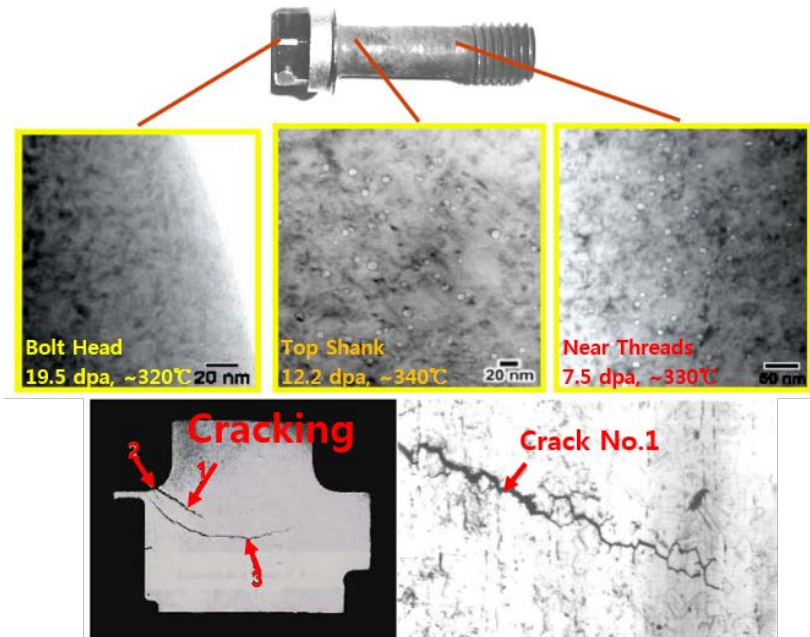
▲ Swelling of 20% CW 316 under neutron irradiation [2]

Possible long-term material degradation issues

- **Radiation induced swelling**
- Transmutations (B, Ni to He / Mn to Fe)
- **Phase stability**



▲ Irradiation Induced degradation of austenitic SS [1]

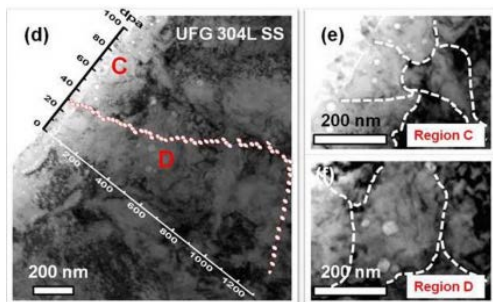
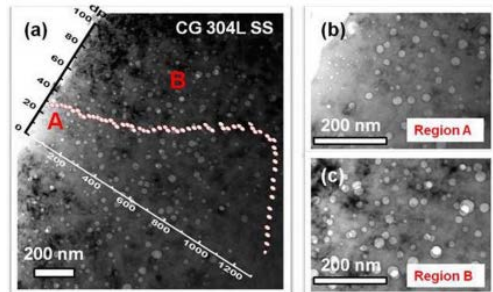
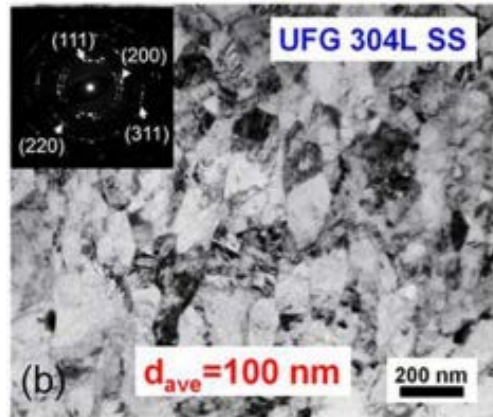


▲ Microstructure of baffle bolt irradiated in Tihange reactor [3]

ARES - Motivation

- [1] C. Sun et al., Sci. Rep. 5 (2015) 7801
- [2] E.H. Lee et al., Phil. Mag. A 61 (1990) 733
- [3] G.R. Odette et al., Annu. Rev. Mater. Res. 38 (2008) 471
- [4] E.J. Pickering et al., Int. Mater. Rev. 61:3 (2016) 183
- [5] L. Tan et al., JOM 68 (2016) 517

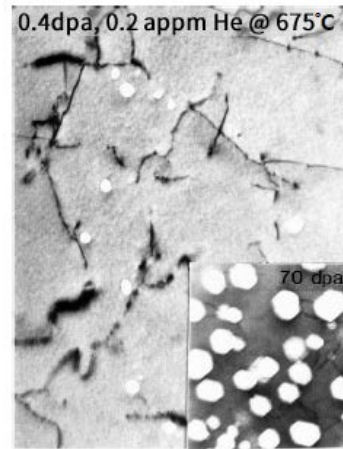
Nano-grain [1]



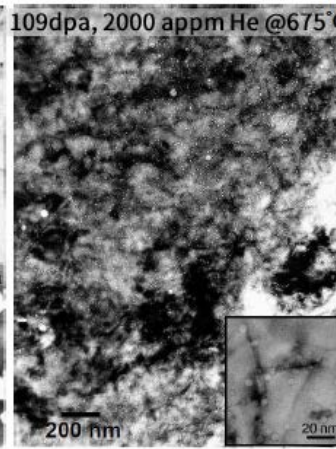
<Potential Sink Sites>

Dislocation + nano precipitates [2]

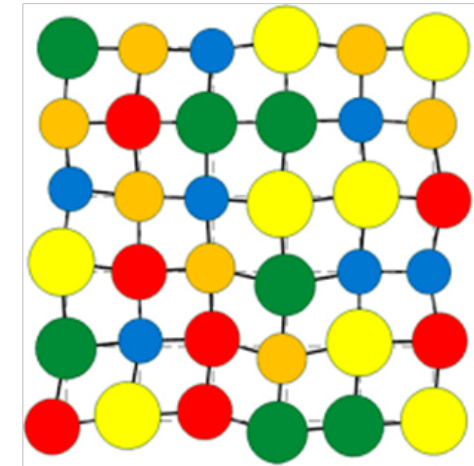
Fe-13Cr-15Ni



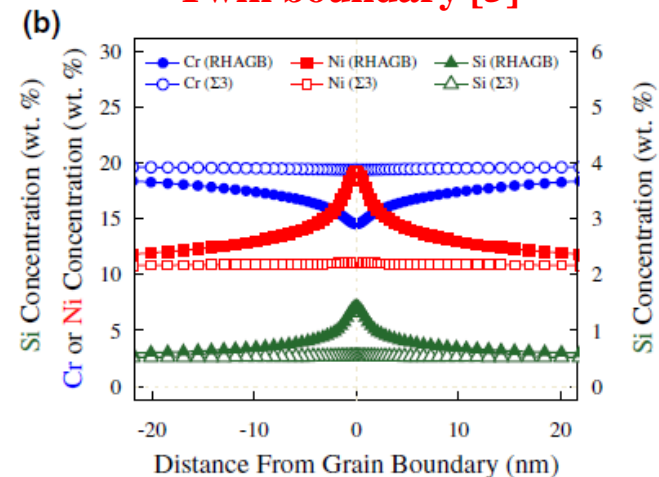
Cold work (P, Si, Ti, C) modified



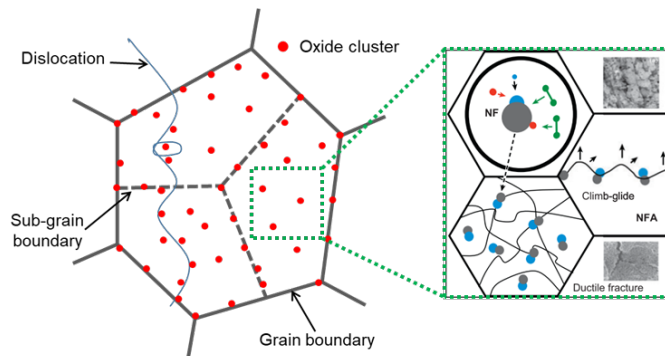
HEA [4]



Twin boundary [5]



FMS or ODS [3]



*Nano Carbide dispersed Advanced radiation RESistant austenitic stainless Steels (ARES)

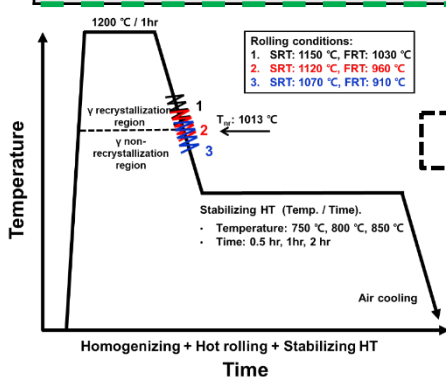
5

Development of advanced radiation resistant austenitic SSs

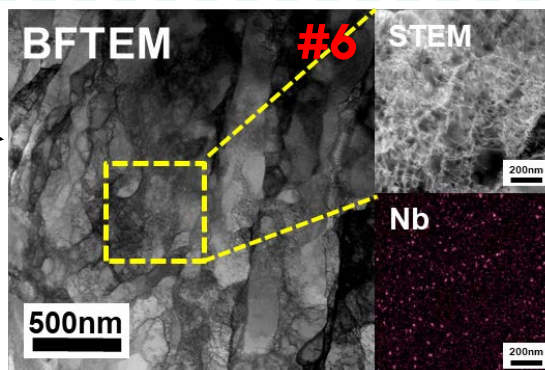
Principal alloy design strategy [1–5]

1. Control the **chemical composition** ► High **resistance to IASCC** (or SCC)
2. Development of new conceptual **thermo-mechanical processing** (TMP) ► Formation of **sink sites**

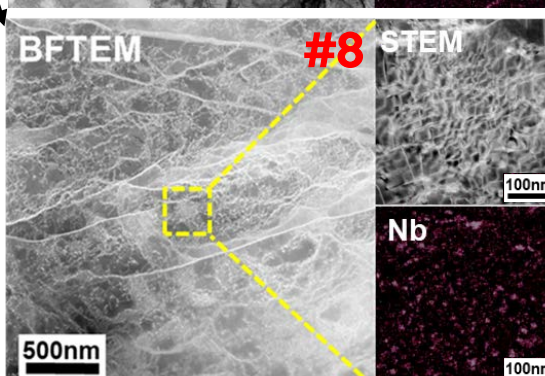
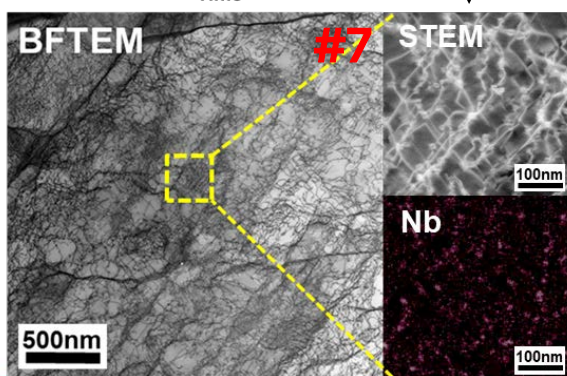
Wt.%	Fe	Cr	Ni	C	Mn	P	S	Si	Nb	Ti	N	Mo
ARES #6	Bal.	24.13	21.07	0.042	1.32	0.0100	0.0020	0.23	0.27	0.023	0.008	-
ARES #7	Bal.	24.03	20.88	0.035	3.41	0.0062	0.0021	0.21	0.45	-	0.010	-
ARES #8	Bal.	24.12	20.94	0.034	3.44	0.0053	0.0022	0.21	0.46	-	0.010	0.77



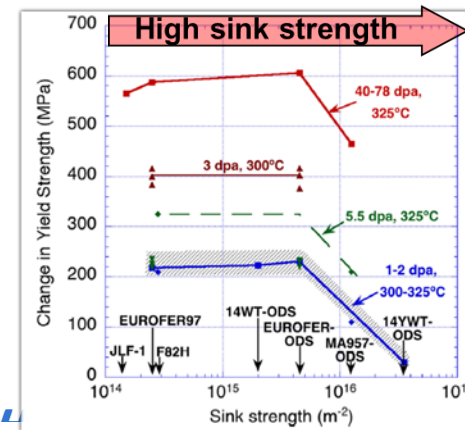
TMP



	Grain size (μm)	Precipitates	
		Mean diameter (nm)	Mean density (X10 ²² m ⁻³)
ARES #6	10.3	8.4	1.1
ARES #7	23.1	7.8	6.8
ARES #8	10.8	5.8	13.2



Our Goal

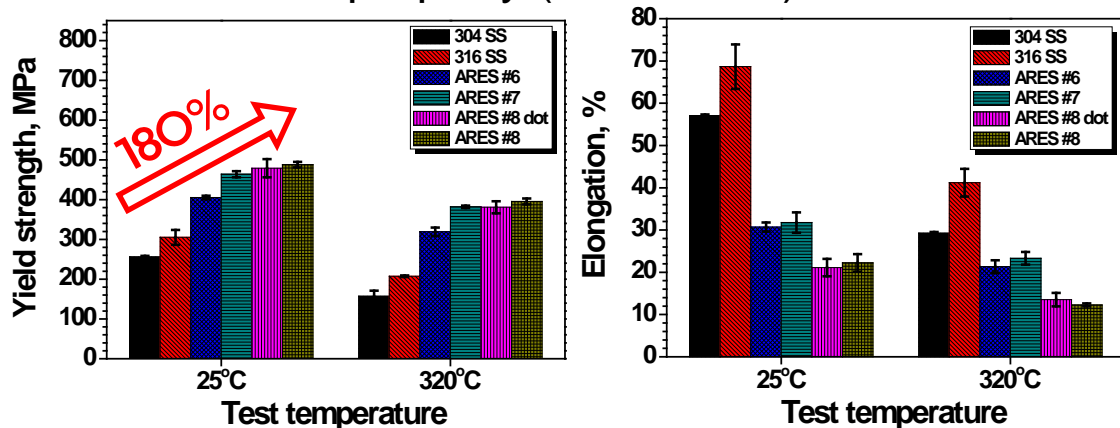


▲ Effect of initial sink strength depending on materials [6]

ARES – Mechanical/Corrosion

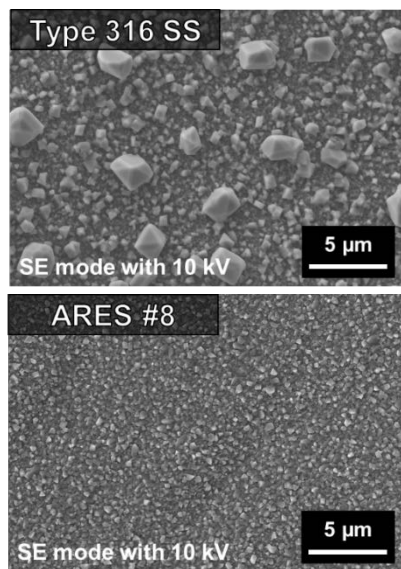
□ Evaluation of mechanical and corrosion properties

● Mechanical property (tensile test)



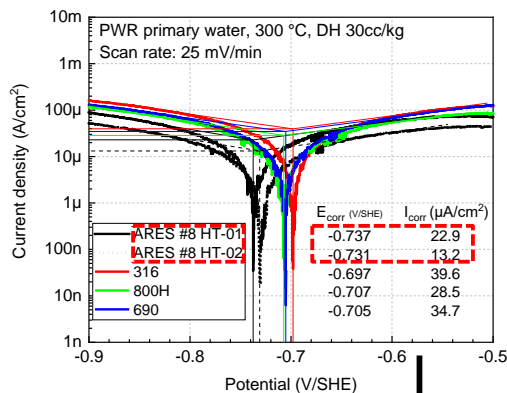
● Corrosion properties

1. SCC test



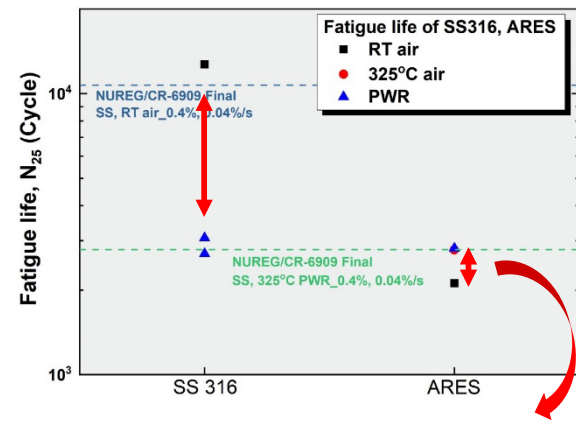
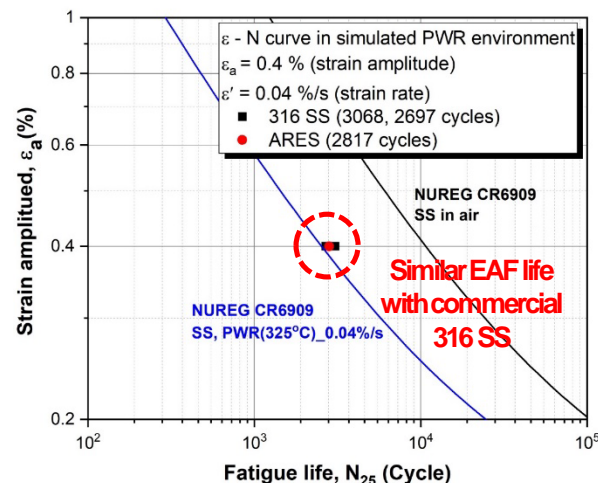
▲ Surface morphology on 316 SS and ARES #8 (400°C and 20 MPa for 1332 h)

2. In-situ electrochemical test



Higher oxidation resistance in ARES

3. EAF test

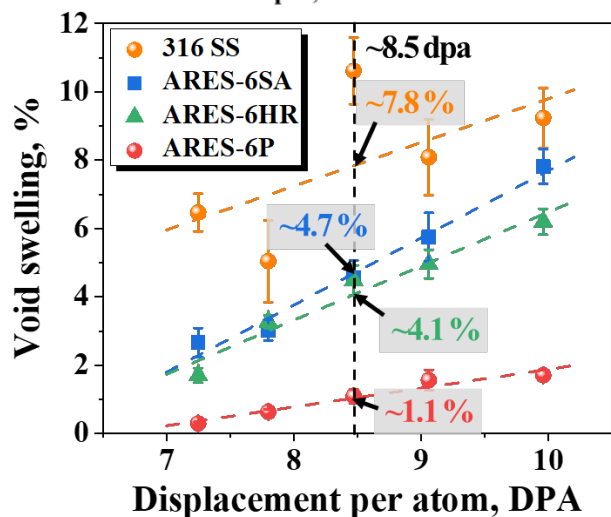
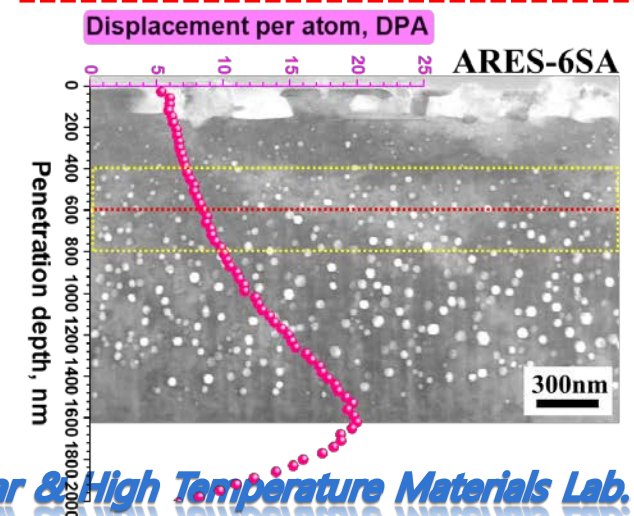
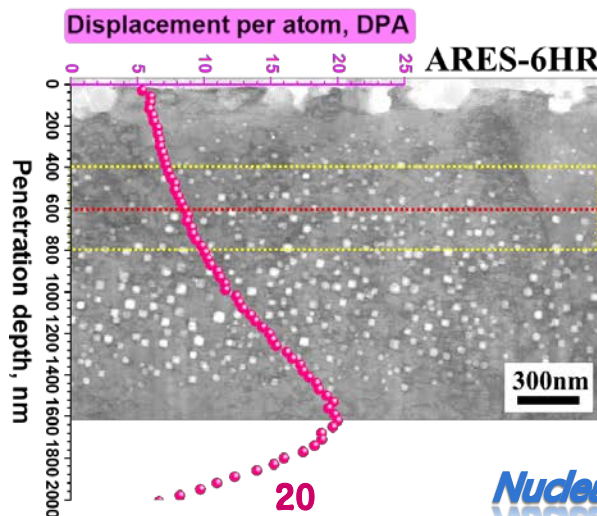
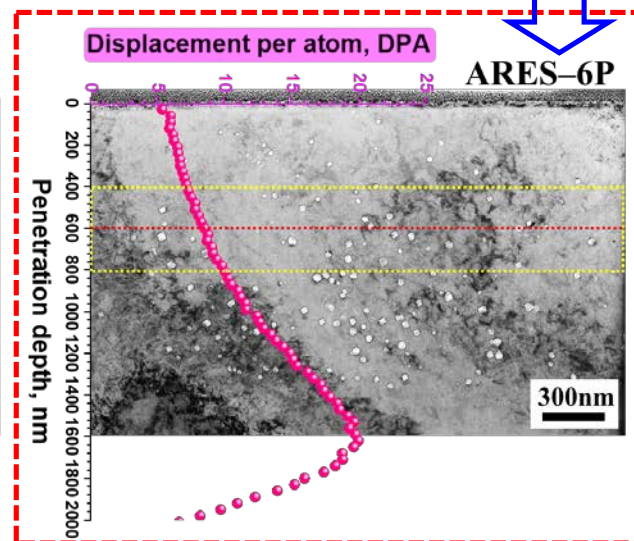
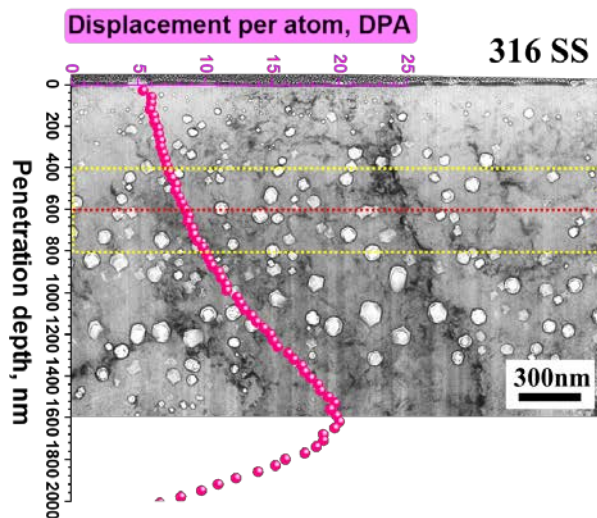
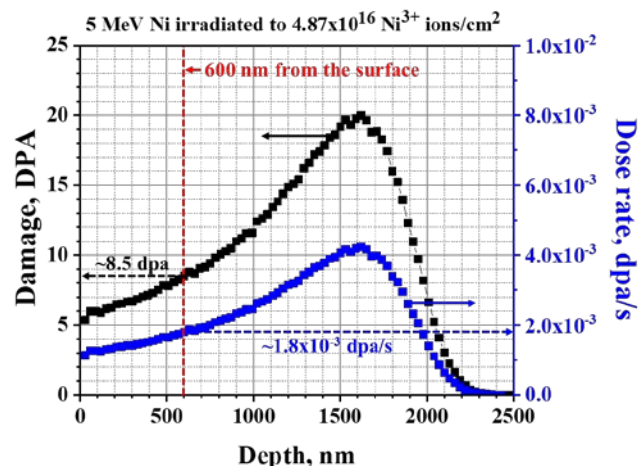


Surface treatment by laser peening to improve the LCF life

Effect of nanosized NbC precipitates on void swelling

- Irradiated by MIT (prof. M.P. Short) / 8.5 dpa

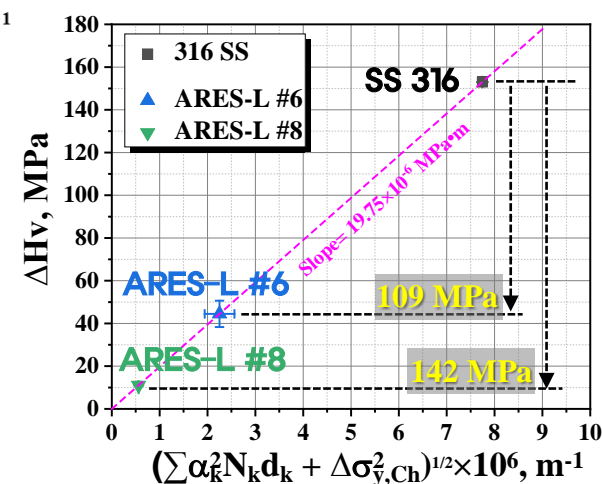
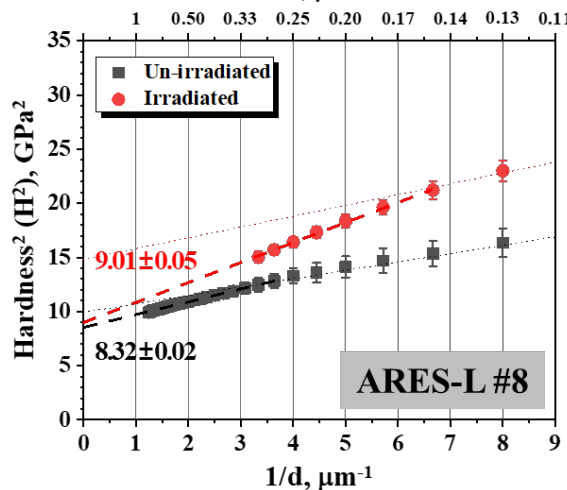
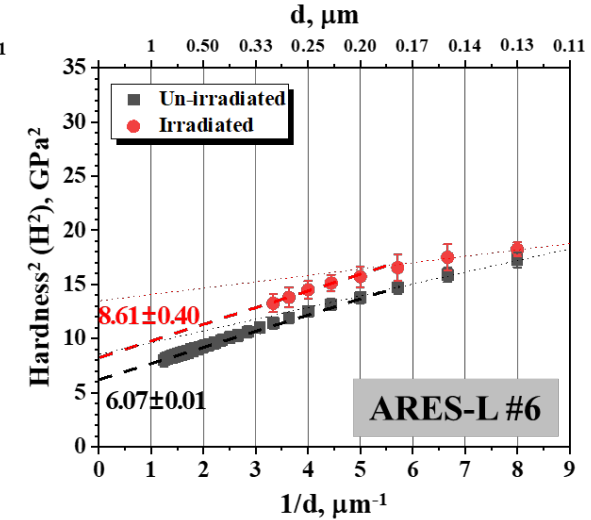
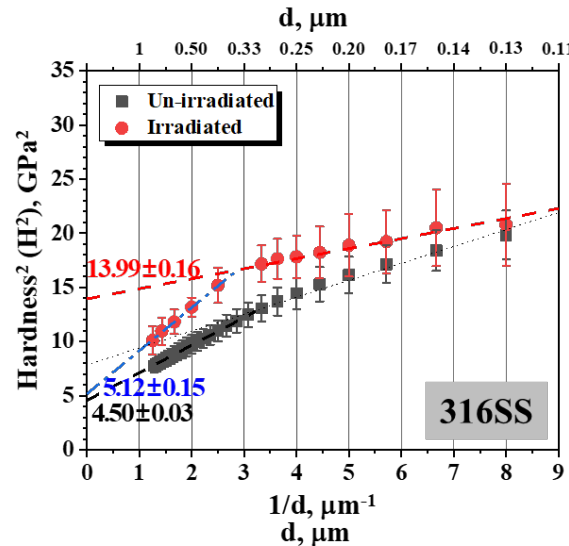
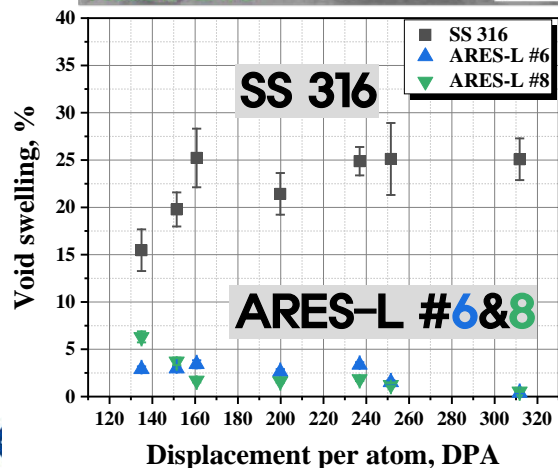
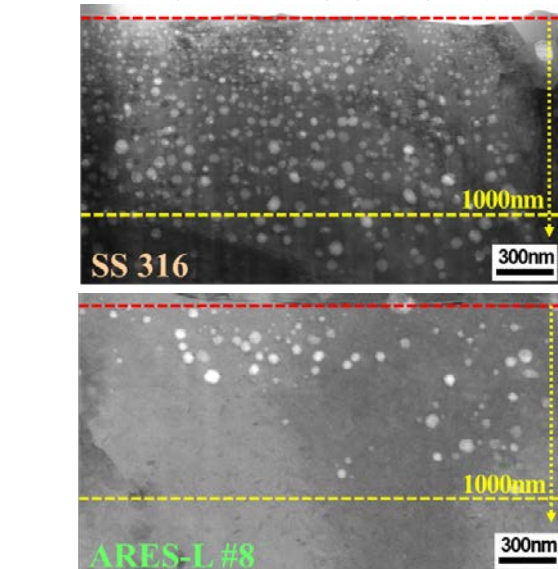
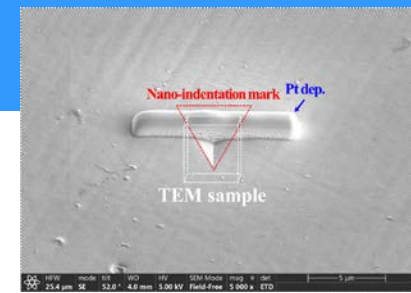
Drastically enhanced void swelling resistance of ARES-6P



ARES – Heavy ion irradiation

□ Radiation hardening resistance

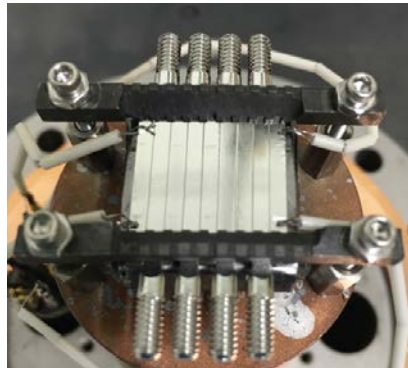
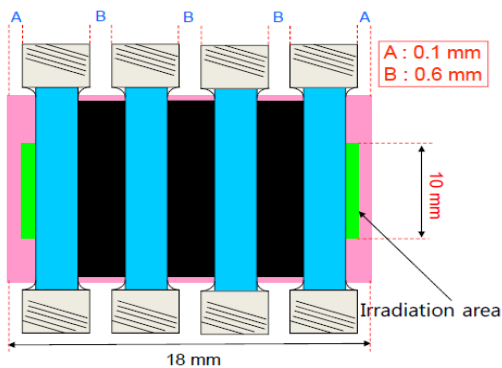
- Irradiated by **Texas A&M** (prof. Lin Shao) / **200 dpa**
- Nano-indentation test



ARES – IASCC resistance

❑ Irradiation-assisted stress corrosion cracking resistance⁹

- Proton irradiation by **MIBL** (Michigan Univ., prof. G. Was)
- Test condition:
 - Damage (5 dpa), Energy (2 MeV), dose rate ($\sim 10^{-5}$ dpa/s), Temp. (360°C)



MIBL

SSRT specimens



Nu_Html



Specimen

Jig

Dummy

Jig

Dummy

Jig

Dummy

Jig

Dummy

Jig

Dummy

Jig

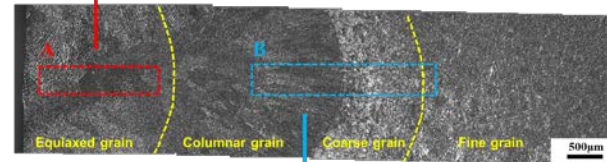
Dummy

Jig

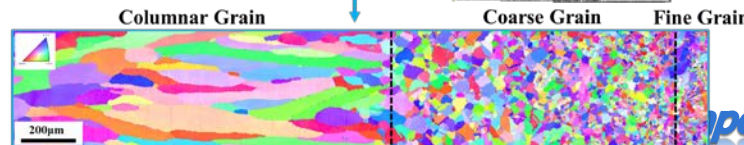
Dummy

Jig

❑ Development of welding procedure for ARES



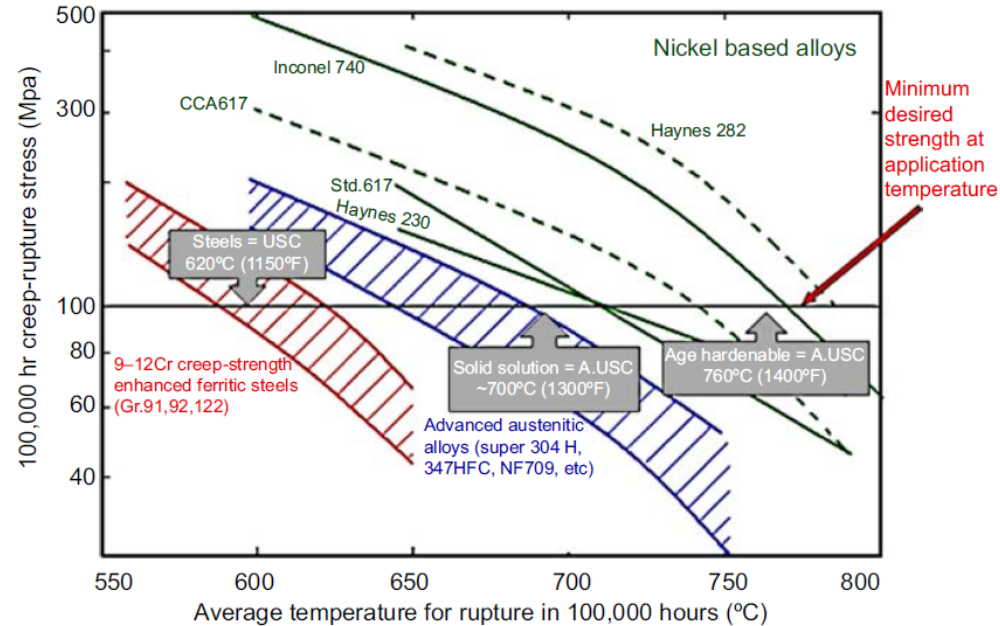
TEM



III. ACES for HTR & Non-Nuclear

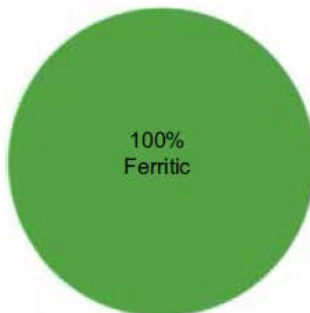
HT materials

- Design temperature criterion: creep rupture life of $>10^5$ h for 100 MPa
- Advanced austenitic SS are catching up Ni-based solid solution strengthened (SSS) alloys

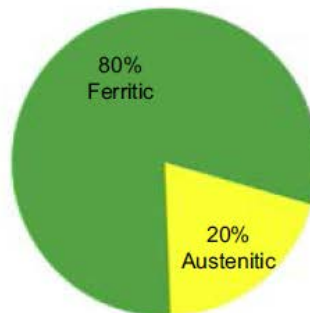


▲ Relative creep rupture strength of steels and nickel alloys [1]

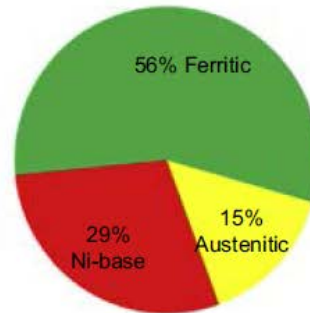
250 bar 540°C / 520°C



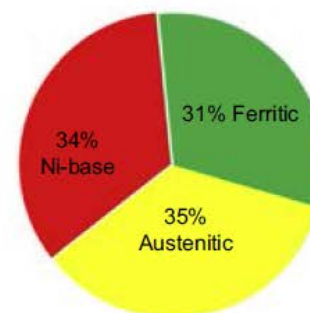
280 bar / 600°C / 620°C



360 bar / 700°C / 720°C



350 bar / 730°C / 760°C



▲ Material fraction in subcritical, supercritical, ultra-supercritical and advanced ultra-supercritical power plants [2]

Alumina-forming alloys (ORNL)

- Typical composition: Fe-(20~32)Ni-14Cr-(2.5~3.5)Al
 - Increasing Ti → increased γ' -Ni₃(Al,Ti) fraction → higher creep life
 - Ti degrades corrosion resistance; minor elements (ZCB) improve

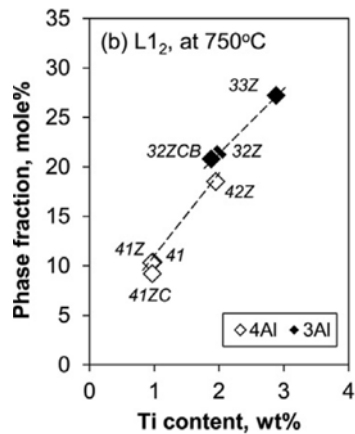
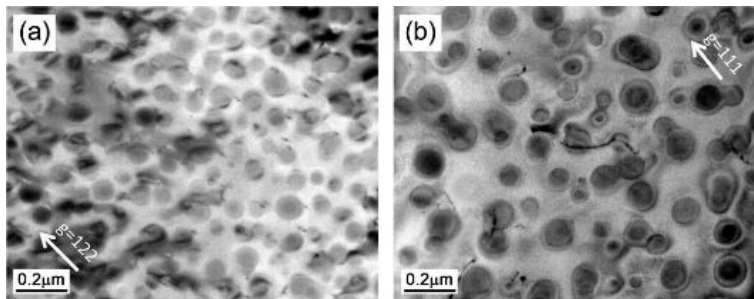


Table 1. Chemical compositions of the alloys studied.

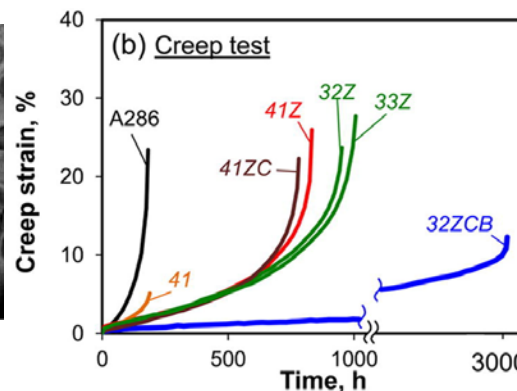
Name	Analyzed composition (wt%)										Remarks
	Fe	Cr	Ni	Al	Si	Nb	Ti	Zr	C	B	
4I	45.73	14.03	32.26	3.96	0.14	2.88	0.98	—	—	—	4Al – 1Ti
4IZ	45.62	14.02	32.23	3.93	0.12	2.81	0.96	0.27	—	—	4Al – 1Ti + Zr
4IZC	45.38	14.03	32.23	3.98	0.14	2.86	0.97	0.29	0.102	—	4Al – 1Ti + Zr, C
42Z	44.32	13.97	32.45	3.91	0.13	2.95	1.95	0.30	—	—	4Al – 2Ti + Zr
32Z	45.29	14.00	32.47	2.95	0.13	2.93	1.97	0.29	—	—	3Al – 2Ti + Zr
33Z	44.23	14.02	32.46	2.98	0.14	2.96	2.88	0.29	—	—	3Al – 3Ti + Zr
32ZCB	45.36	13.99	32.46	2.97	0.14	2.80	1.88	0.29	0.065	0.005	3Al – 2Ti + Zr, C, B
A286	56.2	14.5	25	0.15	0.2	—	2.1	—	0.04	0.006	1.25Mo, 0.3V, 0.2Mn, 0.015P

▲ Composition of alumina-forming alloys studied in Ref. [1]

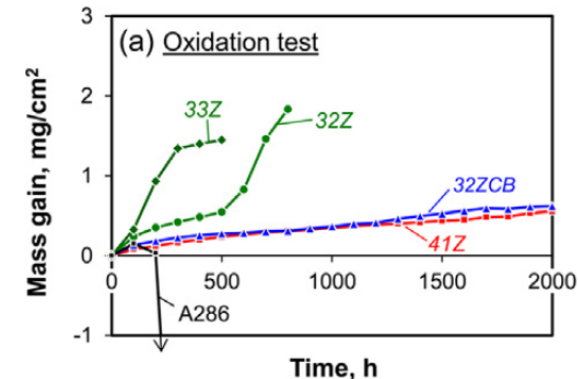
▲ Phase stability of γ' precipitates with Ti content[1]



▲ γ' precipitates after creep testing of (a) 32Z and (b) 32ZCB at 750 °C [1]



▲ Creep test at 750°C and 100MPa [1]



▲ Oxidation in air + 10% H₂O at 800°C [1]

ACES - Approach

High Ti for γ' -Ni₃(Al,Ti)

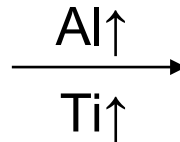
High Al for Al₂O₃



Balanced creep & corrosion resistance

Alumina forming alloys (AFA)

Fe-(20-32Ni)-(14-16Cr)-(2-4Al)-(<2
Ti)-(2-3Nb)+ZCB

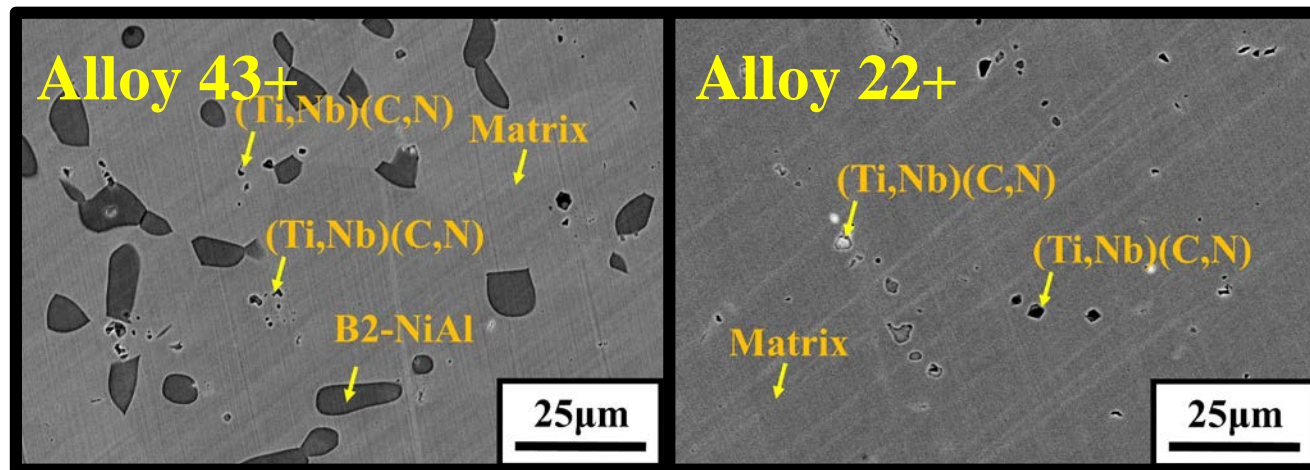


High Al-Ti alloys

Fe-(30-35Ni)-(16-18Cr)-4.
5Al-(2-4Ti)-1Nb+ZCB

SEM analysis

- Coarse B2-NiAl phases with fraction, size and composition similar to cast alloy 43+ SA



▲ SEM-BSE images showing the microstructure of the model alloys

Alloy	Phase	Fe	Ni	Cr	Al	Ti	Nb	Si	Zr
43+	Matrix	Bal.	28.7	18.9	7.9	3.2	0.3	0.4	0.01
	B2-NiAl phase	Bal.	40.3	7.5	23.5	6.6	0.3	0.3	0.04

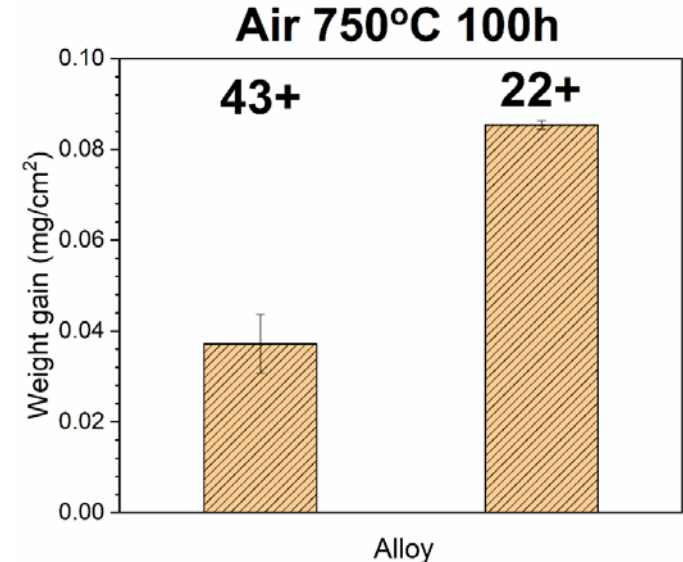
▲ Average composition in at.% of the phases in alloy 43+

Creep condition	Alloys	Creep rupture time (h)
750 °C and 150 MPa	43 SA (cast condition)	270 h
	43+ SA (cast condition)	525 h
	43+ AR (wrought condition)	478 h
	Alumina-forming alloys (with Laves, carbide and γ' -Ni ₃ (Al,Ti) precipitates) – calculated from LMP plot	~ 100 – 300 h
	Alloy HR6W	~ 100 h
	Sanicro 25	~ 1000 h
750 °C and 100 MPa	43 SA (cast condition)	1510 h
	Alumina-forming alloys (with Laves and carbide precipitates)	~ 200 – 2000 h
	Alumina-forming alloys without Ti (with Laves, carbide and γ' -Ni ₃ (Al,Ti) precipitates)	867 h
	Alumina-forming alloys with Ti and beneficial minor elements Zr, C and B (with Laves, carbide and γ' -Ni ₃ (Al,Ti) precipitates)	~ 3000 h
	Alloy HR6W (22Cr-22Fe-7W)	~ 2000 h
	Alloy HR120 (25Cr-37Ni-MWCo)	~3000 h
	Alloy NF709 (20Cr-25Ni-1.5MoNbTiN)	~ 5000 h
	Sanicro 25 (22-Cr-25Ni-4W)	~ 8000 h

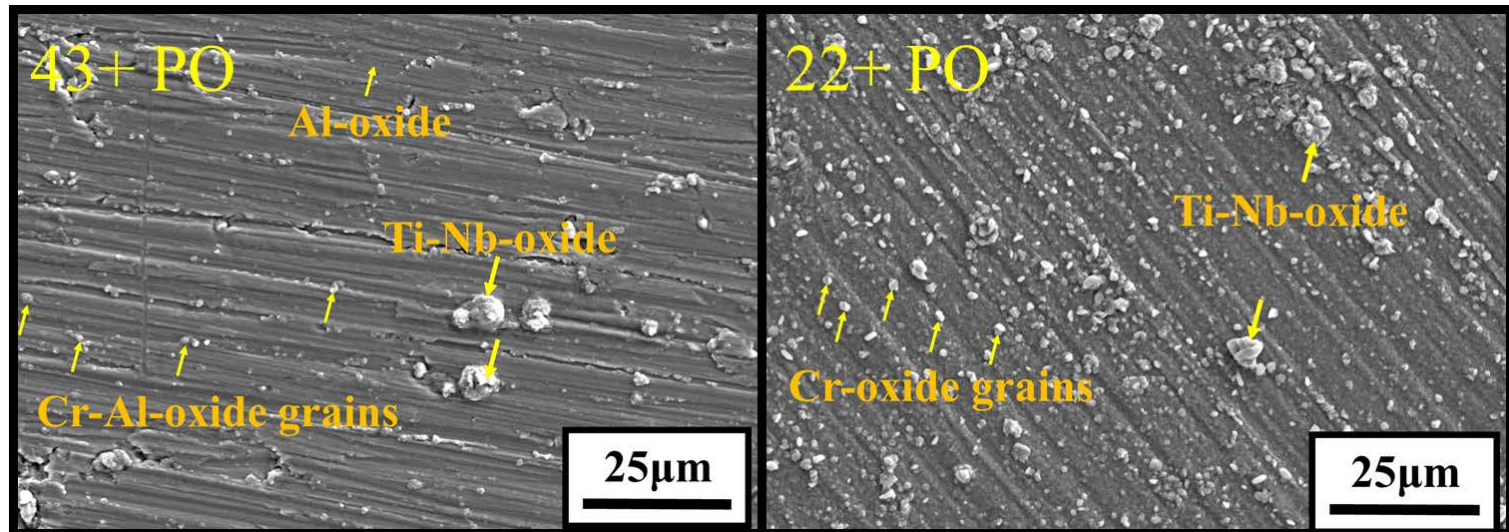
ACES - High temperature oxidation

□ Air oxidation 750°C 100h

- Alloy 43+ → Lower weight gain and Al-oxides on surface
- Alloy 22+ → Cr-rich oxide
- Ti-Nb-oxides from previously Ti-Nb-carbonitrides



▲ Weight gain after oxidation in air at 750°C for 100h

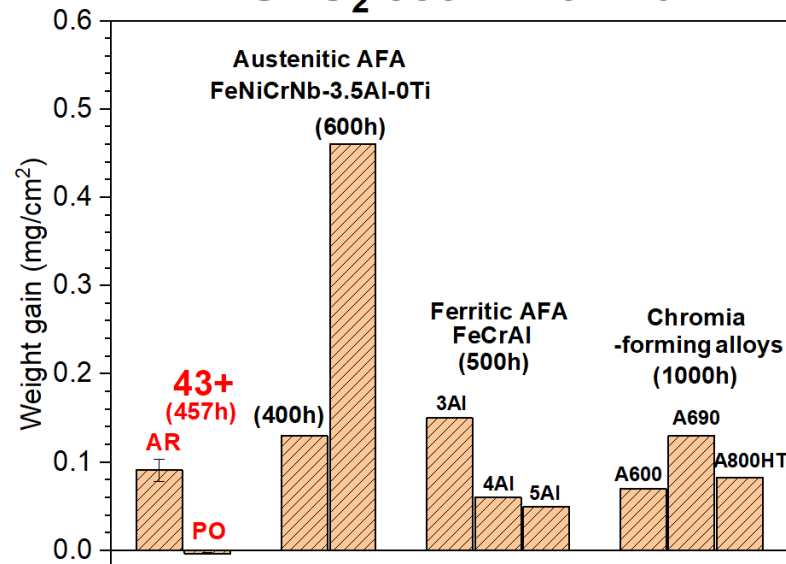


▲ SEM-SE surface images after oxidation in air at 750°C for 100h

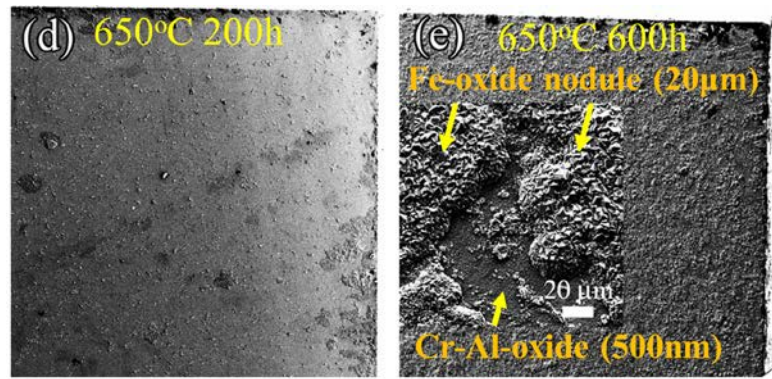
Compared with other alloys

- AFA (3.5Al-3Nb-0Ti) in S-CO₂ → breakaway corrosion (Cr & Al depletion)
- Protective Cr₂O₃ → Higher Cr-content beneficial

SCO₂ 650°C 20MPa

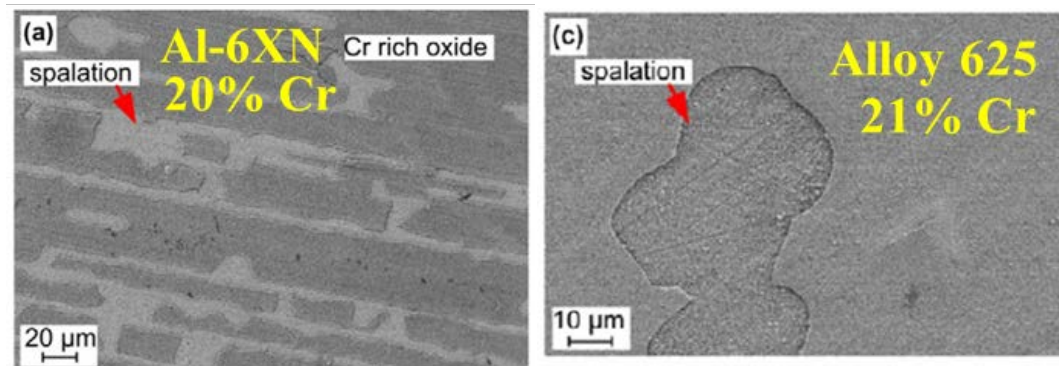


Alumina-forming alloys



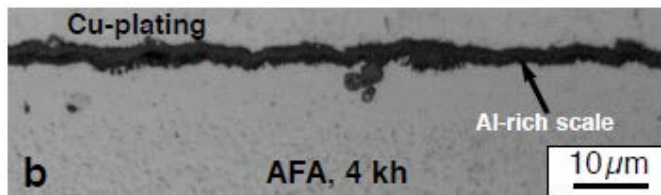
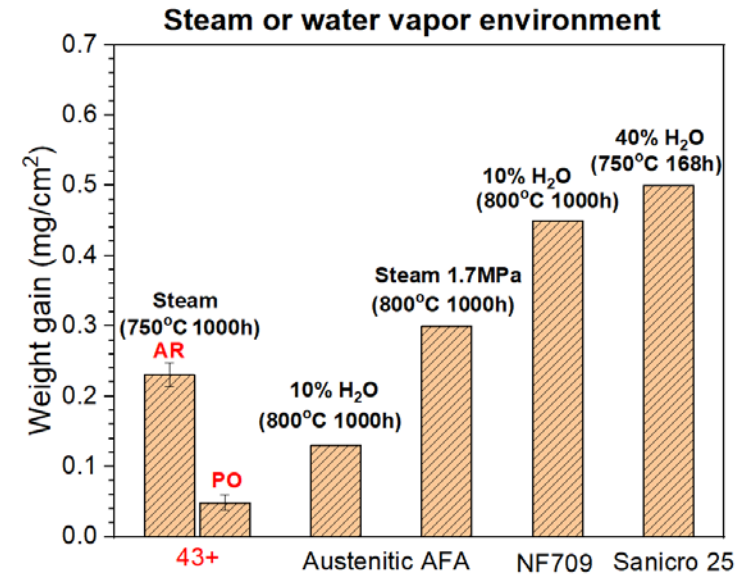
▲ Weight gain and surface morphology of AFA (3.5Al-2.5Nb-0Ti) in S-CO₂ environment at 650°C [1]

Chromia-forming alloys

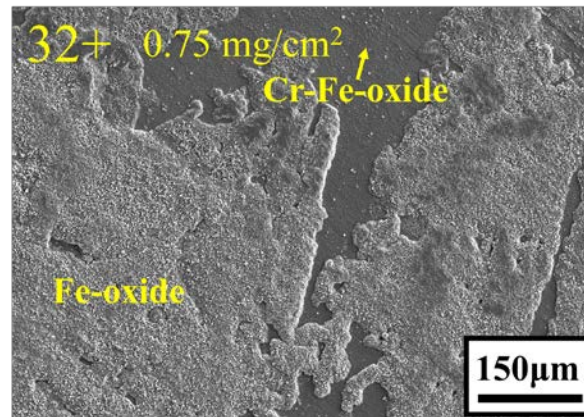


▲ Surface morphology of Al-6XN (Fe-24Ni-20.5Cr) and Alloy 625 (Ni-21.5Cr) alloys in S-CO₂ environment at 650°C [2]

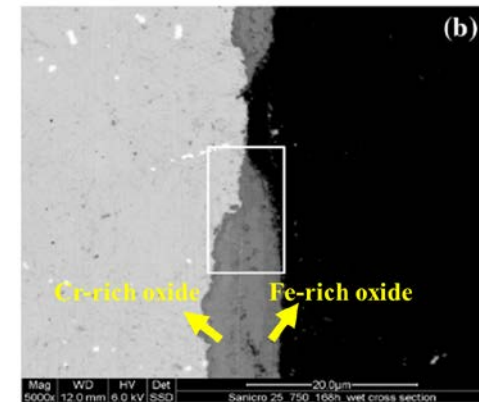
- Compared with other alloys
 - Alumina forming alloys offer better protection in H_2O environments
 - Chromia-forming alloys susceptible to breakaway corrosion



▲ Cross-section of an austenitic AFA after corrosion in steam environment at 550°C and 800°C [1]



▲ Alloy Fe-32Ni-14Cr-3Al-2Ti-1Nb-0.075Zr-0.075C-0.01B in steam at 750°C for 1000h



▲ Cross-section of Sanicro 25 after corrosion in H_2O environment at 750°C for 168h [2]

Summary

❑ ADSS

- Excellent high temperature steam oxidation resistance with large strengthening by B2 phase
- Affordable thermal ageing embrittlement
- Thin tube of $t \sim 0.3$ mm successfully fabricated by cold-pilgering

❑ ARES-L

- High-Cr, High-Ni austenitic SS with large quantity of nanosized NbC precipitates in austenite matrix
- Excellent corrosion resistance in LWR environment
- Excellent swelling resistance up to 200 dpa confirmed by ion irradiation

❑ ACES

- Al and Ti were increased for better oxidation creep resistance compared to ORNL-AFA
- Pre-oxidation of alumina forming alloy(43+) further improved oxidation resistance in air, S-CO₂, and steam.

Energy for Earth !!



Thank you!